On the evolution of the plant phytochrome chromophore

Federica Frascogna[1], Benjamin Ledermann[1], Jana Hartmann[1], Eugenio Pérez Patallo[1], Eckhard Hofmann[2], Nicole Frankenberg-Dinkel[1*]

[1]*Department of Microbiology, Technische Universität Kaiserslautern, 67663 Kaiserslautern, Germany*

[2]*Department of Protein Crystallography, Ruhr Universität Bochum, 44780 Bochum, Germany*

**corresponding author:* nfranken@bio.uni-kl.de*;* phone +49 631 2052353

running head: Phytochrome chromophore biosynthesis in streptophytes

Abstract

Phytochromes are biliprotein photoreceptors present in plants, algae, certain bacteria and fungi. Land plant phytochromes use phytochromobilin (PΦB) as the bilin chromophore. Phytochromes of streptophyte algae, the clade from which land plants evolved, employ phycocyanobilin (PCB), leading to a more blue-shifted absorption spectrum. Both chromophores are synthesized by ferredoxin-dependent bilin reductases (FDBRs) starting from biliverdin IXα (BV). In cyanobacteria and chlorophyta, BV is reduced to PCB by the FDBR phycocyanobilin:ferredoxin oxidoreductase (PcyA), whereas, in land plants, BV is reduced to PΦB by phytochromobilin synthase (HY2). However, phylogenetic studies proved the absence in streptophyte algae of any ortholog of PcyA and the presence of only PΦB biosynthesis related genes (*HY2*). The HY2 of the early diverging streptophyte alga *Klebsormidium nitens* (formerly *Klebsormidium flaccidum*) was already indirectly indicated to be involved in PCB biosynthesis. To provide the direct evidence of an intrinsic FDBR activity of this enzyme, we overexpressed and purified a His_6-tagged variant of *K. nitens* HY2 (KflaHY2) in *E. coli*. In anaerobic bilin reductase activity assays, we found that KflaHY2 is a functional FDBR yielding mostly 3(*Z*)-PCB as the reaction product. Via coupled phytochrome assembly assays, we identified 3(*Z*)-phytochromobilin and 18^1,18^2-dihydrobiliverdin (18^1,18^2-DHBV) as intermediates of the reaction. With the help of site-directed mutagenesis two aspartate residues were identified to be critical for catalysis. Overall, our study gives insight into the evolution of the HY2 lineage of FDBRs.

Introduction

Photosynthesis is arguably one of the most significant biological processes on earth. To efficiently harvest light, photosynthetic organisms possess chlorophyll light-harvesting antennae incorporated in their photosystems. Moreover, some of these organisms are also capable to sense the quality and intensity of the harvested light. To do that, they employ several types of photoreceptors, which are able to absorb photons and to modulate biological activities based on this information (Möglich et al., 2010). Among these photoreceptors, phytochromes can be found in plants, algae, certain bacteria and fungi (Sharrock, 2008). Phytochromes are capable to perceive red and far-red light, by employing open-chain tetrapyrroles as light-sensing chromophores. Phytochrome's chromophore composition is dependent on the organism's habitat. Interestingly, even if phylogenetically closely related, land plants and streptophyte algae employ different bilins in their phytochromes, marking the impact of terrestrialization. Indeed, land plants use the dark blue pigment phytochromobilin (PΦB), whereas streptophyte algae employ the cyan pigment phycocyanobilin (PCB) (Wu et al., 1997). The different bound chromophore leads to a blue shift of the photocycles in the phytochromes of streptophyte algae compared to the ones of land plants. The light-sensing open-chain tetrapyrroles employed in the photoreceptors are all derived from heme. The first step in the biosynthesis of the bilins is the cleavage of the heme macrocycle at the α-methine bridge mediated by heme oxygenases (HOs). This reaction yields the open-chain tetrapyrrole biliverdin IXα (BV), liberating H_2O, CO and Fe^{2+} (Cornejo and Beale, 1988). BV is then subsequently reduced to the specific bilins by a class of enzymes called ferredoxin-dependent bilin reductases (FDBRs) (Figure S1) (Frankenberg et al., 2001; Frankenberg and Lagarias, 2003). In land plants, the enzyme phytochromobilin synthase (HY2) reduces BV in a two-electron reduction at the A-ring 2,3,3^1,3^2-diene system to the dark blue pigment PΦB (**Figure *1***) (Kohchi et al., 2001; McDowell and Lagarias, 2001). In cyanobacteria and chlorophyta, phycocyanobilin:ferredoxin oxidoreductase (PcyA) catalyzes the four-electron reduction of BV to the cyan pigment PCB via the intermediate 18^1,18^2-dihydrobiliverdin (18^1,18^2-DHBV) (**Figure *1***) (Frankenberg and Lagarias, 2003). Interestingly, the streptophyte alga *Klebsormidium nitens* is known to employ PCB in its phytochromes but only possesses a HY2 homolog (Rockwell and Lagarias, 2017). Using coexpression studies, it was suggested that the HY2 of *K. nitens* (named KflaHY2) is able to synthesize PCB and not PΦB, like its higher plant homolog (Rockwell et al., 2017). Here we provide direct biochemical evidence that the recombinant KflaHY2 is able to reduce BV to PCB. In addition, we investigated the reaction in more detail, identifying important catalytic residues. Overall, our data give more insight into the evolution of this interesting enzyme family and also on the evolution of land plants phytochromes.

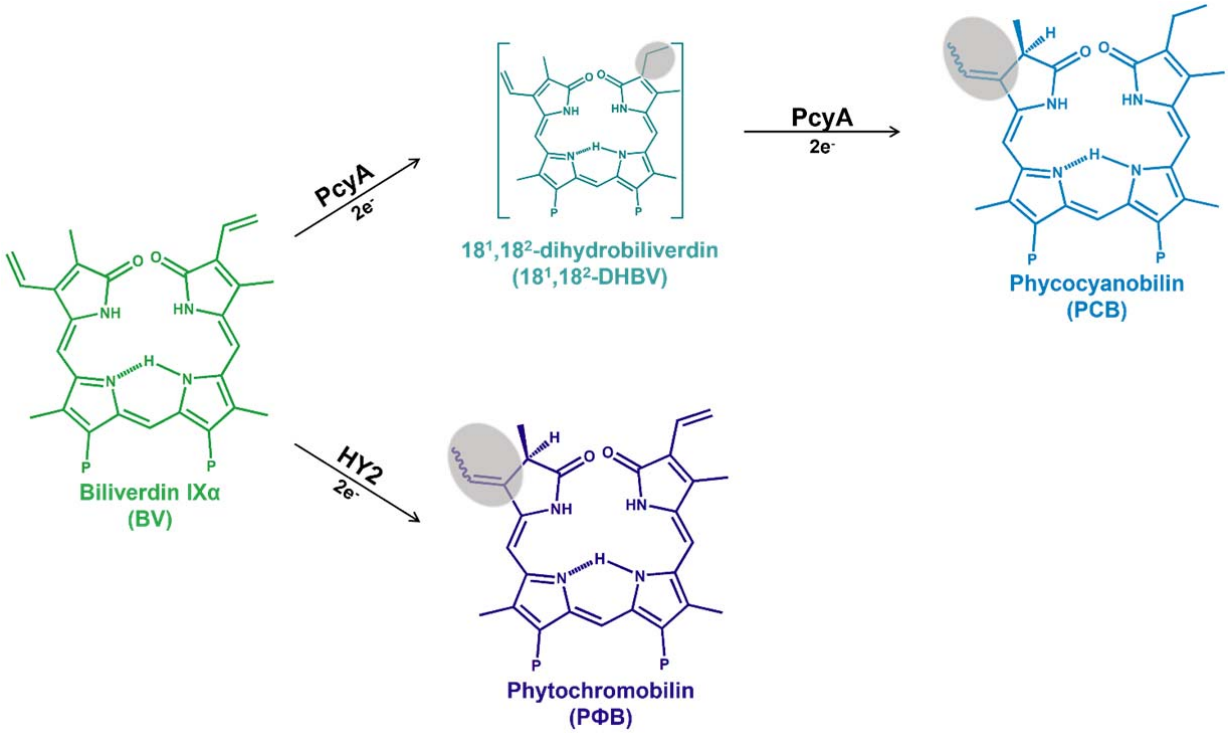

Figure 1 Overview of the reactions catalyzed by the FDBRs HY2 and PcyA. Biliverdin IXα (BV) is the substrate of both FDBRs. "P" indicates the propionate side chains. HY2 catalyzes the two-electron reduction of BV to phytochromobilin (PΦB). PcyA catalyzes the four-electron reduction of BV to phycocyanobilin (PCB) via the intermediate 18^1,18^2-dihydrobiliverdin (DHBV). Sites of reduction are highlighted in grey.

Materials and Methods

Chemicals

All chemicals used in this study were ACS grade or better. The purification resin TALON® Superflow™ was purchased from Cytiva. Most of the components for the anaerobic bilin reductase activity tests were purchased from Sigma, except from biliverdin IXα, which was purchased from Frontier Scientific. Ferredoxin (PetF) and FNR (PetH) were recombinantly expressed and purified as described elsewhere (Dammeyer et al., 2008; Busch et al., 2011). Sep-Pak® C18 Plus Light cartridges were obtained from Waters. HPLC-grade acetone, formic acid and acetonitrile were purchased from VWR Chemicals.

Plasmids

The plasmid pET28a_KflaHY2 was gifted by Prof. J. Clark Lagarias (UC Davis, CA, USA). Site-directed mutants of KflaHY2 were generated in the pET28a_KflaHY2 plasmid using the QuikChange® Lightning kit (Agilent) employing primers listed in Table S1. The variant proteins were produced and purified according to the protocol used for KflaHY2 unless stated otherwise. The full list of employed constructs can be found in Supplemental Materials (Table S2).

Production and purification of recombinant proteins

For the production of recombinant KflaHY2 and variants, 2 L of LB medium containing the appropriate antibiotics was inoculated 1:100 with an overnight culture of *E. coli* BL21(DE3) carrying the respective plasmids. Cells were grown at 37°C and 100 rpm (Innova® 44, New Brunswick Scientific) to an OD_{600} of 0.4-0.6. The temperature was decreased to 17°C and gene expression was induced by the addition of isopropyl-β-D-thiogalactopyranoside (IPTG) to a final concentration of 1 mM (for pET28a_KflaHY2) or 0.5 mM (for pET28a_KflaHY2_N105D, pET28a_KflaHY2_D122N, pET28a_KflaHY2_D242N, pET28a_KflaHY2_N105D_D122N, pET28a_KflaHY2_N105D_D242N). The cultures were incubated under shaking for additional 19 h and harvested at 4°C by centrifugation for 10 min at 17.000 g (Sorvall™ LYNX™ 6000 centrifuge, Rotor T9). The pellets were resuspended in "binding buffer" (20 mM sodium phosphate pH 7.4; 500 mM NaCl). After the addition of a spatula tip of DNaseI (Applichem) and lysozyme (Sigma Aldrich), the suspension was kept on ice for 30 min. The cells were disrupted by sonication for 5 min (Bandelin Sonopuls HD 2200; tip KE76; 5'' pulses, 10'' pauses; cycle 6/10; ≈ 40% power output) and centrifuged for 45 min at 4°C and 50.000 g (Sorvall™ LYNX™ 6000 centrifuge, rotor T29-8). The crude extract was loaded onto a gravity flow column containing 2 mL of TALON® Superflow™ resin (Cytiva). The column was washed with 10 column volumes (CV) of binding buffer and the elution was performed using 4 CV of "elution buffer" (20 mM sodium phosphate pH 7.4; 500

mM NaCl; 500 mM imidazole). Protein containing fractions were pooled and dialyzed overnight against TES-KCl buffer (25 mM TES/KOH pH 7.5; 100 mM KCl; 10% glycerol). The concentration of the purified protein was determined based on its absorbance at 280 nm. Extinction coefficients were calculated as described by Gill and von Hippel (Gill and von Hippel, 1989).

GST-tagged PcyA and GST-tagged mHY2 were produced and purified as described previously (Kohchi et al., 2001; Frankenberg and Lagarias, 2003). Apo-Cph1 and apo-BphP were produced as described elsewhere (Tasler et al., 2005; Fiege and Frankenberg-Dinkel, 2020).

Anaerobic bilin reductase assay

The anaerobic bilin reductase activity assays were performed as described previously with minor modifications (Ledermann et al., 2016). In this study, recombinant ferredoxin PetF from the cyanophage P-SSM2 was used as the electron donor in a final concentration of 1 µM. PetF was reduced using recombinant Ferredoxin-$NADP^+$ reductase (FNR) from *Synechococcus* sp. PCC7002, PetH, at a final concentration of 0.01 µM (Busch et al., 2011). The reaction was started by the addition of a NADPH regenerating system consisting of 65 mM glucose-6-phosphate, 8.2 µM NADP+ and 11 U/ml glucose-6-phosphate dehydrogenase. For the assays employing defined electron equivalents, the NADPH regenerating system was replaced with a NADPH solution of a specific concentration. The photometric measurements were carried out using an Agilent 8453 spectrophotometer. The reaction was stopped by the dilution 1:10 in ice cold 0.1% TFA. Products were isolated via solid phase extraction using Sep-Pak® C18 Plus Light cartridges (Waters) and freeze-dried using an Alpha 2-4 LSC plus lyophilizer (Martin Christ GmbH).

HPLC analyses

The products of the anaerobic bilin reductase assays were analyzed using an Agilent 1100 series chromatograph equipped with a Luna® 5µm reversed phase C18-column (Phenomenex). The mobile phase consisted of 50% (v/v) acetone and 50% (v/v) 20 mM formic acid at a flow rate of 0.6 mL/min. Reaction products were identified by comparison of the retention time with known standards as well as whole spectrum analysis of the elution peaks. Products of interest were collected directly at the outlet of the UV-Vis detector, frozen at -80°C and freeze-dried.

Coupled phytochrome assembly assays

In vitro chromophore assembly of the phytochromes Cph1 and BphP with different bilins was carried out using the lysate of a pET_*cph1* or a pASK_*bphP* overexpression after centrifugation and filtration. The assembly was tested employing 50 µL lysate incubated

150 either with 40 μM standard bilin or with 4 μL of bilin solutions of unknown concentration for 30
151 min at room temperature, in the dark. Afterwards the volume was adjusted to 500 μL with
152 PBS. Absorbance spectra were recorded after incubation for 3 min with red light (636 nm –
153 Pr spectrum) and after incubation for 3 min with far red light (730 nm for Cph1; 750 nm for
154 BphP – Pfr spectrum). Difference spectra were calculated by the subtraction of the Pfr from
155 the Pr spectrum.

156 Phytofluor analyses

157 Phytofluor formation was evaluated via fluorescence measurements (Murphy and Lagarias,
158 1997). Briefly, 50 μL lysate of a pET_*cph1* or a pASK_*bphP* overexpression, after
159 centrifugation and filtration, was incubated with 4 μL of the KflaHY2_N105D reaction product,
160 for 30 min, at room temperature, in the dark. Afterwards the volume was adjusted to 500 μL
161 with PBS. Fluorescence spectra were recorded using a Jasco FP-8300 spectrofluorometer.

Results

KflaHY2 catalyzes the reduction of BV to PCB

It has been known for quite some time that the phytochromes of streptophyte algae use PCB as their chromophore instead of the PΦB found in higher plants phytochrome (Wu et al., 1997; Rockwell et al., 2017). Nevertheless, the streptophyte alga *K. nitens* possesses an FDBR homolog to higher plant HY2. KflaHY2 has 39% amino acid sequence homology to the HY2 of *Arabidopsis thaliana*, and experiments conducted by Rockwell *et al.* suggest that PCB is the enzymatic product of its reaction. In order to biochemically investigate this, the reductase was recombinantly overproduced in *E. coli* and purified by affinity chromatography. The activity of the purified protein was tested in an anaerobic bilin reductase activity assay (Figure 2).

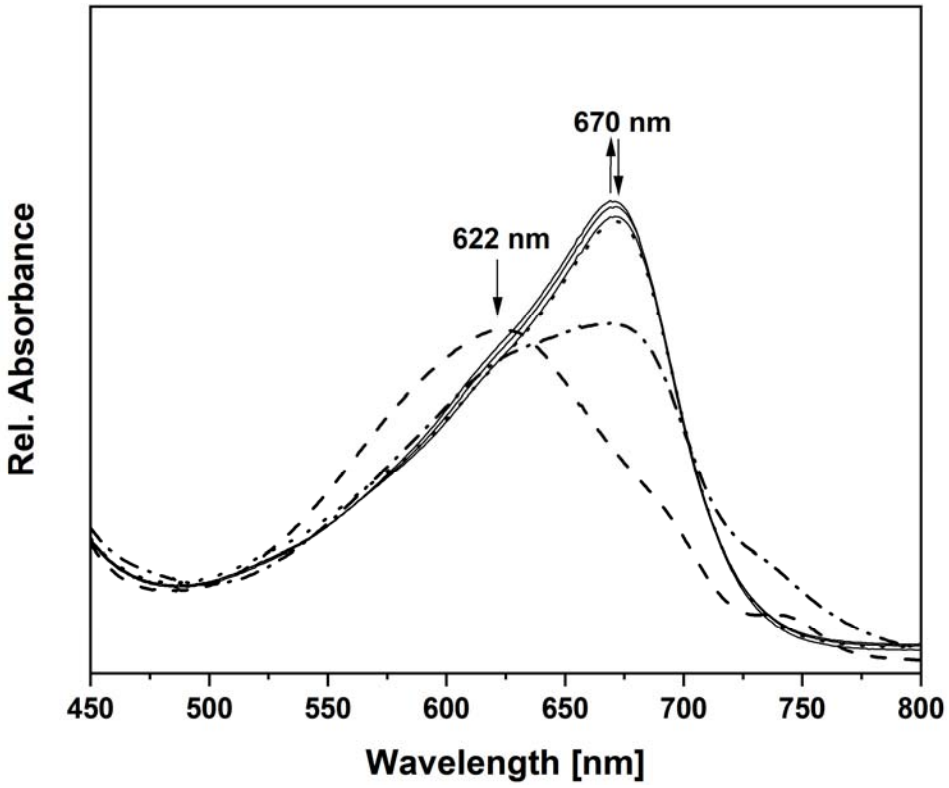

Figure 2 Time-resolved UV-Vis spectra of an anaerobic bilin reductase activity test of recombinant KflaHY2 employing BV as the substrate. Total reaction time was 5 min and spectra were recorded every 30s. The course of the spectra is marked by arrows. For reasons of clarity, only relevant spectra are shown. The dashed spectrum was acquired without starting the reaction. The dotted-dashed spectrum represents the first acquired after starting the reaction. The dotted curve represents the end spectrum.

Interestingly, the reductase and the substrate formed an intense turquoise colored complex with an absorbance maximum at 622 nm, suggesting that the reductase was folded correctly and was able to bind BV (Figure 2). The presence of a shoulder at ~ 750 nm indicates the

184 presence of BV in its protonated form (Frankenberg and Lagarias, 2003; Tu et al., 2004).
185 After the reaction was started, the absorbance decreased instantly. Moreover, a rapid
186 formation of a product with an absorbance maximum at 670 nm, which can be linked to the
187 formation of PCB, was observed. Subsequent HPLC analyses, employing the reaction
188 products of PcyA as standards, revealed that KflaHY2 forms 3(*Z*)-PCB as the main reaction
189 product (**Figure *3***).
190

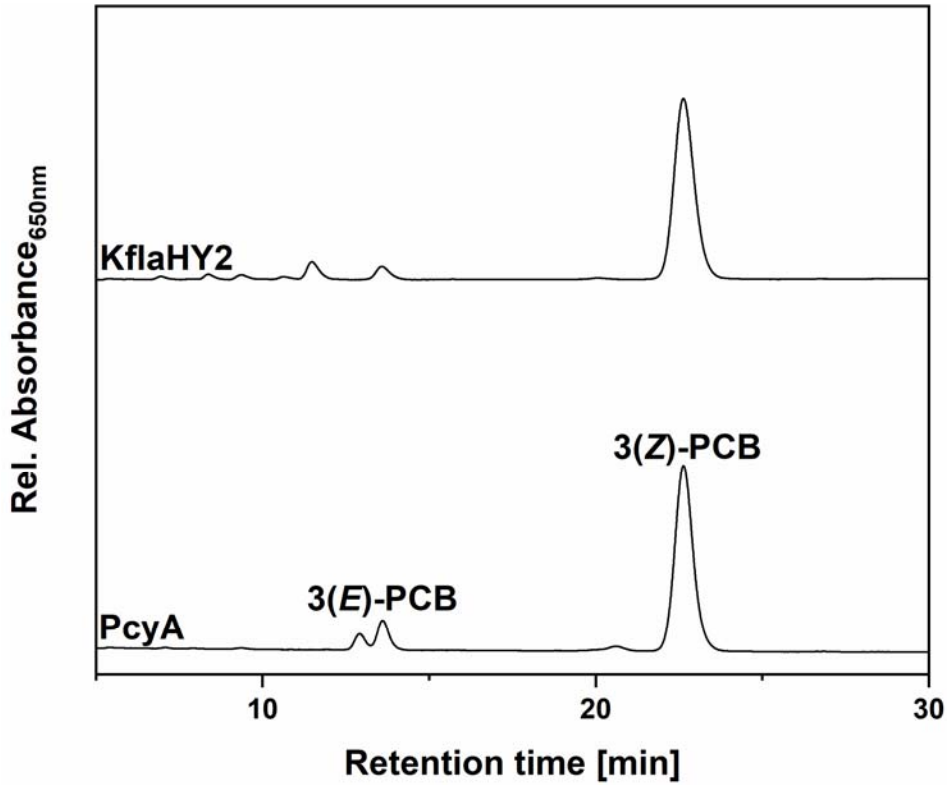

191

192 **Figure 3** HPLC analyses of the reaction products of KflaHY2 with BV as substrate. The products were analyzed
193 using a reversed-phase 5 µm C18 Luna column (Phenomenex) as stationary phase. The mobile phase consisted
194 of 50% (v/v) acetone and 50% (v/v) 20 mM formic acid flowing at 0.6 mL/min. Products of an anaerobic turnover
195 of BV to PCB mediated by PcyA served as standards. Absorbance was continuously measured at 650 nm.

196

197 KflaHY2 reaction can proceed via two intermediates

198 As the KflaHY2 reaction product PCB is a tetrahydro-BV, the reaction should proceed via a
199 two-electron reduced intermediate: either the A-ring reduced PΦB, or the D-ring reduced
200 18^1,18^2-DHBV. Intermediates of the reaction were isolated using the products of an
201 anaerobic bilin reductase activity assay conducted with one electron equivalent of NADPH.
202 HPLC analyses of the products showed that KflaHY2 forms two intermediates (**Figure *4*** –
203 marked as “Inter 1” and “Inter 2”).

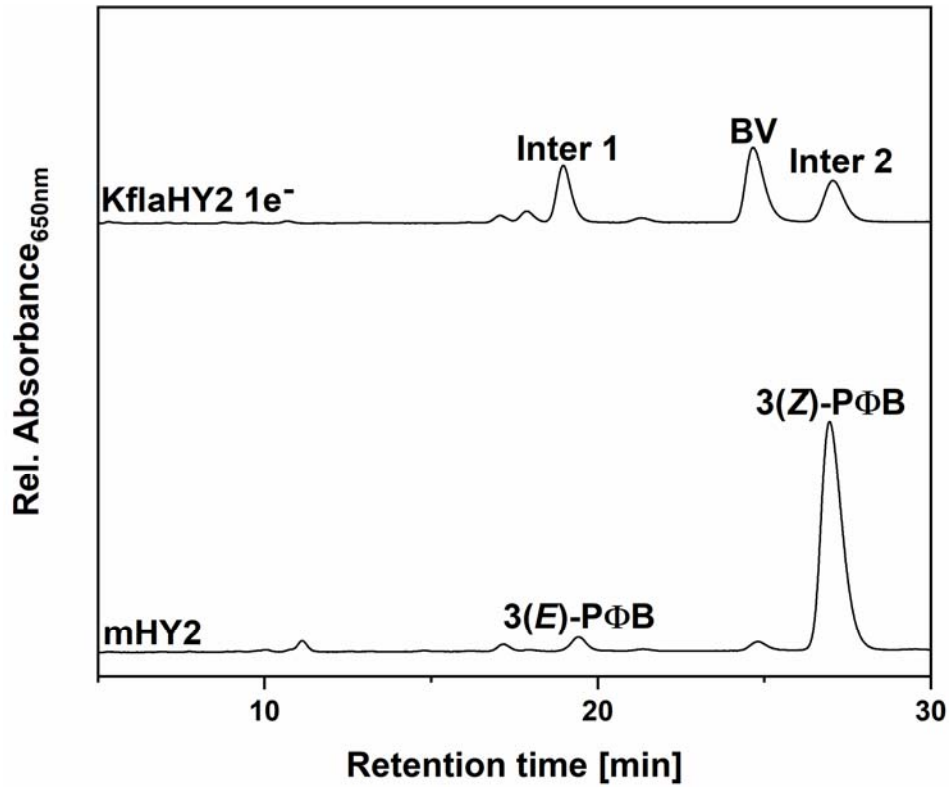

Figure 4 HPLC analyses of the reaction products of an anaerobic activity assay employing equimolar amounts of KflaHY2 and BV with one electron equivalent of NADPH. Products were resolved using a reversed-phase 5 µm C18 Luna column (Phenomenex) as stationary phase and a mixture of 50% (v/v) acetone and 50% (v/v) 20 mM formic acid as mobile phase. The products of an anaerobic turnover of BV to PΦB mediated by HY2 derived from *A. thaliana* were used as standards. Absorbance was continuously measured at 650 nm.

The intermediates possessed the same retention times as the products 3(*E*)-PΦB (~ 19 min) and 3(*Z*)-PΦB (~ 27 min) of the recombinant reductase HY2 from *A. thaliana* (mHY2). However, 18^1,18^2-DHBV, the intermediate of the cyanobacterial PcyA reaction towards PCB, and 3(*E*)-PΦB are roughly characterized by the same retention time. Therefore, "Inter 1" could have been either of the two (Frankenberg and Lagarias, 2003).

The intermediates formed by KflaHY2 are 18^1,18^2-DHBV and 3(*Z*)-PΦB

To confirm the nature of the intermediates identified by HPLC analyses, coupled phytochrome assembly assays of the isolated intermediates with the apo-phytochromes Cph1 from *Synechocystis* sp. PCC 6803 and BphP from *Pseudomonas aeruginosa* were conducted (Figure 5A). Cph1 finds its natural chromophore in PCB, while BphP uses BV. However, phytochromes are also able to accommodate different bilins as long as they possess the same A-ring configuration as the natural chromophore. Thus, Cph1 is able to bind bilins possessing an ethylidene group at the A-ring, whereas BphP only binds bilins with an A-ring endovinyl group (Li and Lagarias, 1992; Tasler et al., 2005). Apo-Cph1 incubated with "Inter 1" did not produce a photoactive adduct since no characteristic difference

226 spectrum was obtained, indicating the lack of the ethylidene group at the A-ring C3 side
227 chain (Figure 5A – dashed line) (Xu et al., 2019). This led to the conclusion that "Inter 1"
228 could not be 3(*E*)-PΦB. Incubation of apo-Cph1 with "Inter 2" (Figure 5A – dotted line) led to
229 a difference spectrum like it was obtained for the incubation of Cph1 with 3(*Z*)-PΦB (Figure
230 5A – solid line). These results, as well as the results of the HPLC analyses (Figure 4), prove
231 that "Inter 2" is 3(*Z*)-PΦB.
232

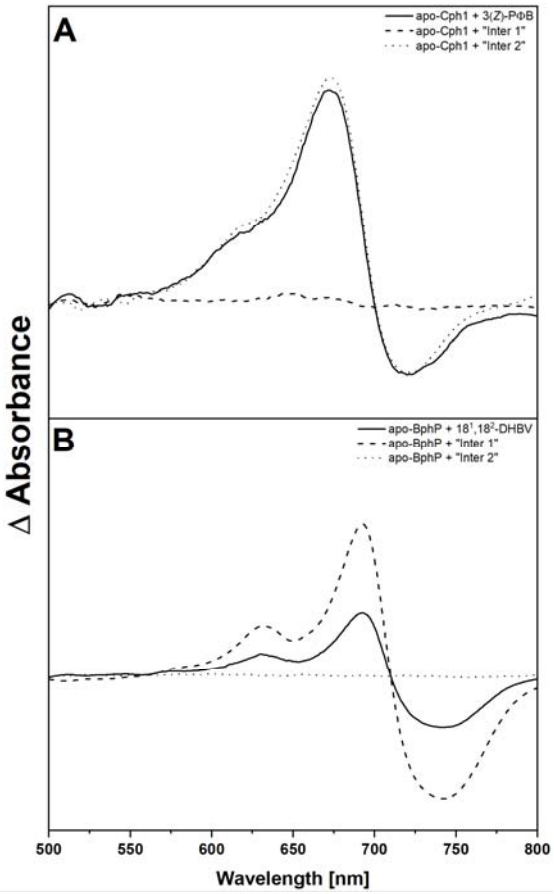

233

234 **Figure 5** Red-far red-light induced difference spectra of coupled phytochrome assembly assays employing the
235 intermediates of the KflaHY2 reaction. Absorbance spectra were recorded after incubation for 3 min with red light
236 (636 nm – Pr spectrum) and after incubation for 3 min with far red light (730 nm for Cph1; 750 nm for BphP – Pfr
237 spectrum). Difference spectra were calculated by the substraction of the Pfr from the Pr spectrum. All calculated
238 difference spectra were smoothed applying a 20 pt. Savitzky-Golay filter. A. Coupled phytochrome assembly
239 assays employing apo-Cph1 and "Inter 1" (dashed line); apo-Cph1 and "Inter 2" (dotted line); apo-Cph1 and 3(*Z*)-
240 PΦB (solid line) B. Coupled phytochrome assembly assay employing apo-BphP and "Inter 1" (dashed line); apo-
241 BphP and "Inter 2" (dotted line); apo-BphP and 18^1,18^2-DHBV (solid line).

242

243 On the other hand, "Inter 2" failed to form a photoactive adduct with apo-BphP (Figure 5B –
244 dotted line), whereas, "Inter 1" formed a photoactive adduct with apo-BphP with a difference
245 spectrum (**Figure *5***5B – dashed line) similar to the difference spectrum obtained by the
246 incubation of BphP with 18^1,18^2-DHBV (**Figure *5***5B – solid line). This revealed that "Inter 1"
247 is indeed 18^1,18^2-DHBV.

To clarify whether the intermediates are only artifacts of the *in vitro* assay or if they are actually suitable in KflaHY2-catalyzed BV reduction, both compounds were used as substrates for KflaHY2 in anaerobic bilin reductase activity assays. Subsequent HPLC analyses revealed that both intermediates are transformed to mostly 3(*Z*)-PCB (Figure 6).

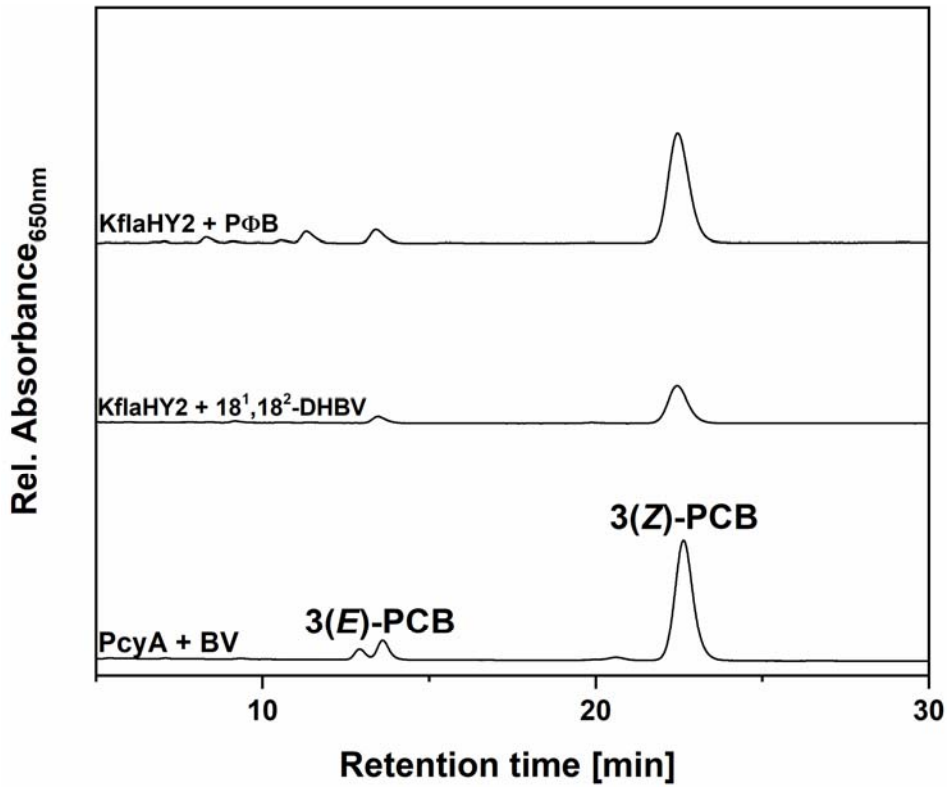

Figure 6 HPLC analyses of the reaction products of activity tests employing 3(*Z*)-PΦB and 18^1,18^2-DHBV as substrates for KflaHY2. Products were analyzed using a 5 µm reversed-phase C18 Luna column (Phenomenex) as stationary phase. The mobile phase consisted of 50% (v/v) acetone and 50% (v/v) 20 mM formic acid flowing at 0.6 mL/min. Reaction products of a PcyA mediated reduction of BV to PCB were used as standards. Absorbance was continuously measured at 650 nm.

Asp^{122} and Asp^{242} are essential for the catalytic activity

In order to gain further insight on the unusual behavior of KflaHY2 and to learn about the evolution of HY2, an amino acid sequence alignment employing different FDBRs was constructed (Figure S2). Three residues caught our attention: Asn^{105}, Asp^{122} and Asp^{242}. KflaHY2 Asn^{105} represents the homolog to *Synechocystis sp.* PCC 6803 PcyA His^{88}, which was proven to be involved in protonation and substrate positioning in the active site (Hagiwara et al., 2010). The substitution of the His to an Asn is not unusual since it can also be found in other FDBRs like PebA, PebB and PebS. On the other hand, land plants HY2s show an Asp in the corresponding position which was also proven to be essential for substrate positioning in *Arabidopsis thaliana* HY2 and involved in catalysis in *Solanum*

lycopersicum HY2 (SlHY2) (Tu et al., 2008; Sugishima et al., 2020). KflaHY2 Asp^{122} finds a homolog in all the FDBRs except for the ones from land plants. In PcyA and PebS, it is located in the central β-sheet of the binding pocket and was shown to be the initial proton donor (Hagiwara et al., 2006; Busch et al., 2011). Finally, Asp^{242} finds a homolog in Asp^{256} of *A. thaliana* HY2, Asp^{256} of *S. lycopersicum* HY2 (SlHY2), Asp^{206} of PebS and Asp^{219} of *Guillardia theta* PEBB. All of these Asp residues were shown to be involved in the reduction of the A-ring 2,3,3^1,3^2-diene system (Tu et al., 2008; Busch et al., 2011; Sommerkamp et al., 2019; Sugishima et al., 2020). On the basis of these considerations, site-directed mutagenesis was performed. To investigate the influence of ionization on catalysis, Asp^{122} and Asp^{242} were replaced by asparagine residues whereas Asn^{105} was replaced by an aspartate residue. Moreover, two double variants were generated. In particular, one was constructed for KflaHY2 to resemble a plant HY2, the other to prove the presence of two Asp residues is enough for reducing BV to PCB. The activity of the purified variant enzymes was investigated *in vitro* via FDBR assays and subsequent HPLC analyses (Figure 7).

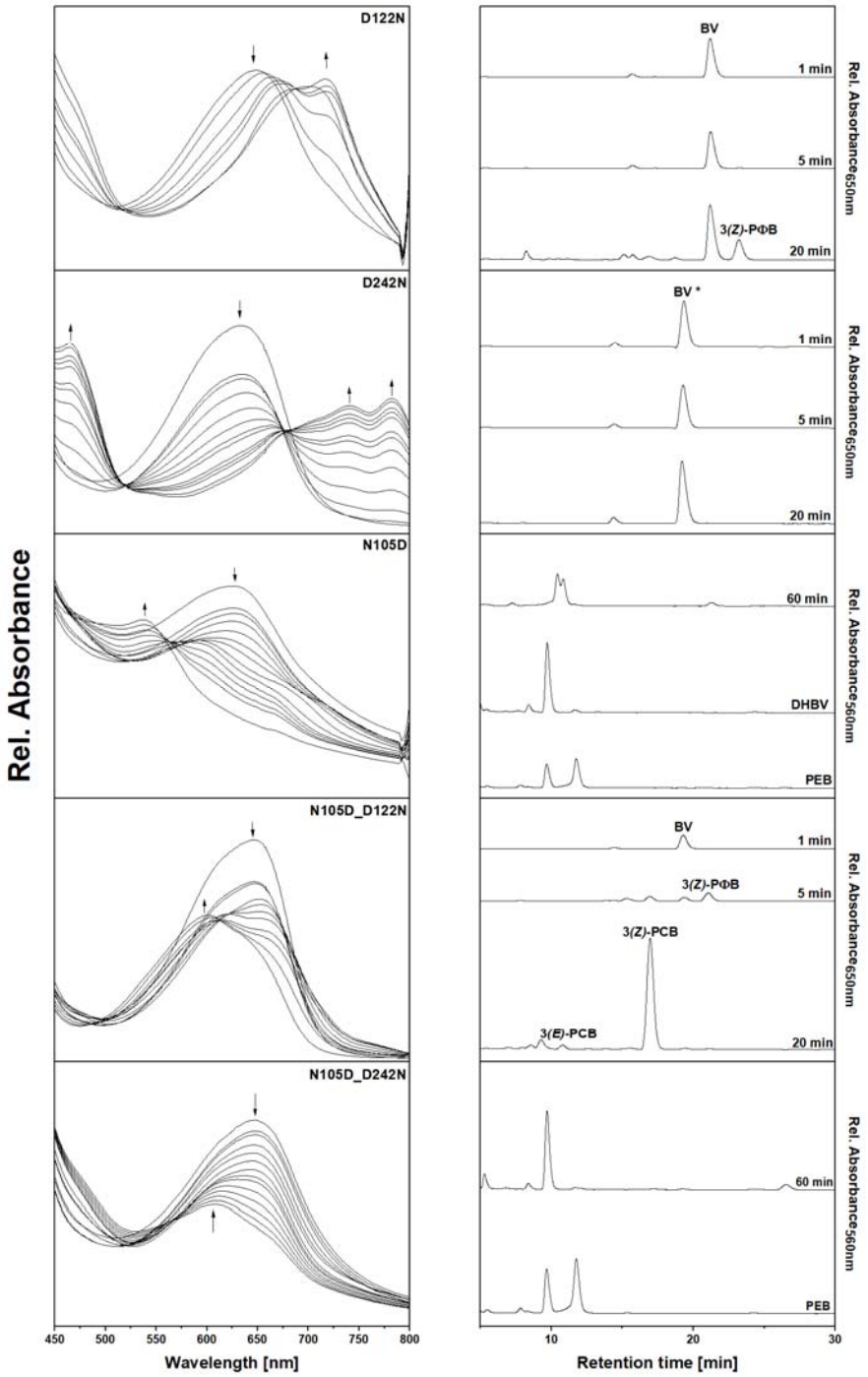

Figure 7 Activity assay and characterization of reaction products of recombinant KflaHY2 variants. A. UV-Vis spectra of the anaerobic FDBR Assay performed using KflaHY2 variants and BV as the substrate. Total reaction time was 20 minutes for KflaHY2_D122N, KflaHY2_D242N, KflaHY2_N105D_D122N and 60 min for KflaHY2_N105D, KflaHY2_N105D_D242N. Spectra were recorded every 30 seconds. For reasons of clarity, only relevant spectra are shown. The arrow indicates the course of absorbance during the reaction. B. HPLC elution profiles of the reaction products of KflaHY2 variants. The stationary phase consisted in a Luna 5µm reversed phase C18 column (Phenomenex). The mobile phase consisted of a mixture of 50% (v/v) acetone and 50% (v/v) 20mM formic acid flowing at 0.6 mL/min. Absorbance was continuously measured at 560 or 650 nm. BV shows change in the retention time due to substitution of the mobile phase between the different HPLC measurements (*).

297 The D122N variant was able to bind BV and use it as a substrate, since the formation of a
298 peak at ~ 720 nm was observed (Figure 7A – D122N). Intermediates were isolated from the
299 reaction mix at certain time points and analyzed via HPLC. Time-course HPLC analyses
300 revealed the formation of small amounts of 3(*Z*)-PΦB after 5 min from the start of the
301 reaction (Figure 7B – D122N). This variant partially retains the capability to reduce BV A-ring
302 but is at all impaired in reducing the D-ring, thus proving the importance of D122 for D-ring
303 reduction.
304 The D242N variant still retained the ability to bind BV but failed in its reduction. The increase
305 of the absorption at ~ 460, ~ 740 and ~ 790 nm suggested the formation of the radical BVH•
306 (Figure 7A – D242N) (Tu et al., 2004; Tu et al., 2008; Busch et al., 2011). The HPLC elution
307 profiles were compatible with BV, therefore confirming the inactivity (Figure 7B – D242N).
308 This result is coherent with what was found for mHY2_D256N and SlHY2_D263N indicating
309 the importance of this residue for BV reduction (Tu et al., 2008; Sugishima et al., 2020).
310 The N105D variant showed an unexpected behavior. The assay was initially performed for
311 20 min but strangely revealed the formation of a violet-colored product with a peak ~ 570 nm,
312 suggesting production of either phycoerythrobilin (PEB) or 15,16-dihydrobiliverdin (15,16-
313 DHBV) (data not shown). In order to potentially accumulate more of this violet compound, we
314 decided to let the reaction run for a longer time, 60 min. This second assay showed the
315 formation of a final product with an absorbance peak at ~ 540 nm (Figure 7A – N105D).
316 Time-based HPLC analyses revealed that the bilin produced after 5 min from the start of the
317 reaction was indeed PCB, whereas a pattern compatible with the unidentified compound and
318 mostly 3(*Z*)-PCB was obtained for the 20 min product (data not shown). As for the final 60
319 min product, HPLC analysis revealed a double peak with the retention time of 10.5 and 10.8
320 min, not matching the retention time of any known bilin and therefore leading to uncertainty
321 (Figure 7B – N105D). To identify the unknown bilin, its integration in the phytochromes Cph1
322 and BphP was evaluated. PEB and 15,16-DHBV lack the C15-16 double bond required for
323 the photoconversion of the phytochrome between the two isoforms. Therefore, phytochromes
324 binding bilins lacking the C15-16 double bond are locked in the red-light absorbing form. In
325 this condition, there is no complete de-excitation of the bilin, leading to the formation of a
326 fluorescent product named phytofluor (Murphy and Lagarias, 1997). The bilin product
327 isolated from the reaction catalyzed by KflaHY2_N105D was then incubated in parallel with
328 the two apo-phytochromes and fluorescence was measured. The formation of a
329 characteristic phytofluor was only observed for the incubation with apo-Cph1, thus
330 suggesting the product is PEB (Figure 8).

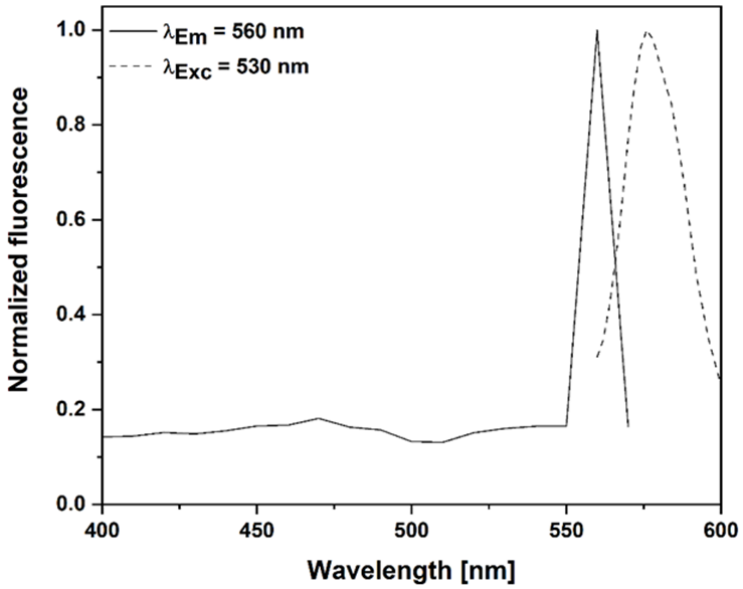

Figure 8 Fluorescence spectra of the apo-Cph1-KflaHY2_N105D reaction product adduct. The isolated bilin produced by KflaHY2_N105D was incubated for 30 min in the dark with the lysate of a pET_*cph1* overproduction. Excitation spectra was obtained at 530 nm. Fluorescence emission was recorded after excitation at 560 nm.

The double variant N105D_D122N, constructed to mimic a plant HY2, surprisingly retained the native activity, revealing the conversion of BV to PCB instead of the hypothesized $2e^-$ reduction to PΦB (Figure 7 – N105D_D122N). This result led to the hypothesis that the presence of two aspartate residues in the active site, even if in different position than in the native enzyme, is enough for the reduction of BV to PCB. To further investigate it, the double variant N105D_D242N was also generated. Interestingly, performing the assay for 60 min revealed the formation of a pink product with an absorbance at ~ 600 nm (Figure 7A – N105D_D242N). Via HPLC analysis, the final product was discovered to be 3(*E*)-PEB (Figure 7B – N105D_D242N), thus showing a different activity than expected.

Discussion

The evolution of land plants finds its roots in streptophyte algae (de Vries and Archibald, 2018). Studies on this clade are particularly significant since they could enlighten the process of colonization of land by embryophytes (Delwiche and Cooper, 2015). Streptophyte algae can mostly be found in freshwater habitats but genera of the Chlorokybophycaeae and Klebsormidiophyceae can also thrive on land. Recent research suggests that freshwater lifestyle paved the way for a pre-adaptation to the terrestrial environment (Becker and Marin, 2009). As photosynthetic organisms, both land plants and streptophyte algae endow complexes to efficiently sense and harvest light. Among them, phytochromes are bilin-photoreceptors which control growth and development (Hu et al., 2013). The impact of terrestrialization is evident when considering the different phytochromes' bilin composition of the two genera. Land plants use PΦB as the bilin chromophore whereas streptophyte algae

were shown to employ PCB (Wu et al., 1997; McDowell and Lagarias, 2001; Rockwell et al., 2017). These bilins are characterized by different spectral properties: while PCB absorbs orange and red light (λ_{PCB} = ~ 620 - 670 nm), PΦB absorbs far-red light ($\lambda_{P\Phi B}$ = ~ 660 - 685 nm). Both chromophores are synthesized by a class of enzymes named FDBRs. In land plants, PΦB is synthesized by the FDBR HY2; in cyanobacteria and chlorophyta, PcyA synthesizes PCB. In streptophyte algae, phylogenetic studies proved the existence of a HY2 homolog (Hori et al., 2014). However, previous research indirectly pointed out to a PcyA-like activity of streptophyte algae HY2 (Rockwell et al., 2017). In this study, we found that the HY2 of *Klebsormidium nitens* is indeed a functional FDBR, which, in contrast to the phylogenetic classification as an HY2, catalyzes the reduction of BV to PCB. Furthermore, we identified 18^1,18^2-DHBV and 3(*Z*)-PΦB as intermediates occurring under the chosen assay conditions. These results were somehow unexpected, as they lead to the conclusion that KflaHY2 can mediate the reduction of BV to PCB employing two different reaction mechanisms. One pathway implies the reduction of BV D-ring leading to 18^1,18^2-DHBV, which is then reduced at the A-ring to PCB. The other starts with the reduction of BV A-ring ethylidene group to 3(*Z*)-PΦB. The D-ring exovinyl group of 3(*Z*)-PΦB is then reduced, leading to PCB. The formation of 3(*Z*)-PΦB as an intermediate during PCB biosynthesis is also tying well with previous phytochrome studies in the Zygnematophycea *Mesotaenium caldariorum* (Wu et al., 1997). Additionally, according to evolution, one could argue the preferred way is the latter, meaning that the HY2 of land plants lost the ability to perform the last reduction step, to yield 3(*Z*)-PΦB as the final product. In this context, studies on even closer relatives to embryophytes and early diverging land plants could provide the answer.

Using a site-directed mutagenesis approach, we also proved that the residues Asp^{122} and Asp^{242} are of crucial importance. This conclusion fitted with the hypothesis made based on sequence homology among FDBRs. To further corroborate the thesis, a model structure of KflaHY2 was obtained using AlphaFold (Jumper et al., 2021). The obtained model structure showed an overall similar folding of KflaHY2 to other FDBRs. Additionally, two structure alignments were constructed using PyMOL: one with the crystal structure of the HY2 of *Solanum lycopersicum*, with which KflaHY2 shares high sequence homology, the second with the crystal structure of PcyA of *Synechocystis* sp. PCC 6803 (SynPcyA), catalyzing BV to PCB reduction as KflaHY2 (Figure 9) (Hagiwara et al., 2006; DeLano, 2020; Sugishima et al., 2020). The obtained alignments revealed a higher similarity of the KflaHY2 active site to the one of SlHY2. As a matter of fact, the two bottom β-sheets residues completely superimpose to each other, whereas only a slight shift in the upper aspartate residue is appreciable (Figure 9A). On the other hand, the relative residue in SynPcyA, Asp^{220}, is facing outside of the active site and was proven to be uninvolved in catalysis, whereas the A-ring reducing residue was found to be Asp^{105} (Figure 9B) (Hagiwara et al., 2006). However, if this

residue is conserved among KflaHY2 and SlHY2, the same is not true for the other. Indeed, based on the biochemical data, we propose KflaHY2 Asp^{122} to be involved in BV D-ring reduction, but this corresponds to Asn^{140} in SlHY2. The additional proton donor of SlHY2 was found to be Asp^{123}, which, on the other hand, corresponds to an asparagine residue (Asn^{105}) in KflaHY2. Contrastingly, in SynPcyA, the reduction of the D-ring exovinyl group was proven to be catalyzed by the residue Glu^{76}, which does not find a homolog in KflaHY2 (Hagiwara et al., 2006). The specificity of reduction is furthermore influenced by the substrate binding mode of BV which was shown to be flipped in the PebB/HY2 lineage of FDBRs (Sommerkamp et al., 2019; Sugishima et al., 2020). We propose this is also true for KflaHY2 as two critical amino acid residues responsible for the stabilization of BV in the ZZZssa flipped binding mode are conserved. Overall, the data indicate that the ability of KflaHY2 to synthesize PCB has evolved independently from the biosynthesis catalyzed by PcyA.

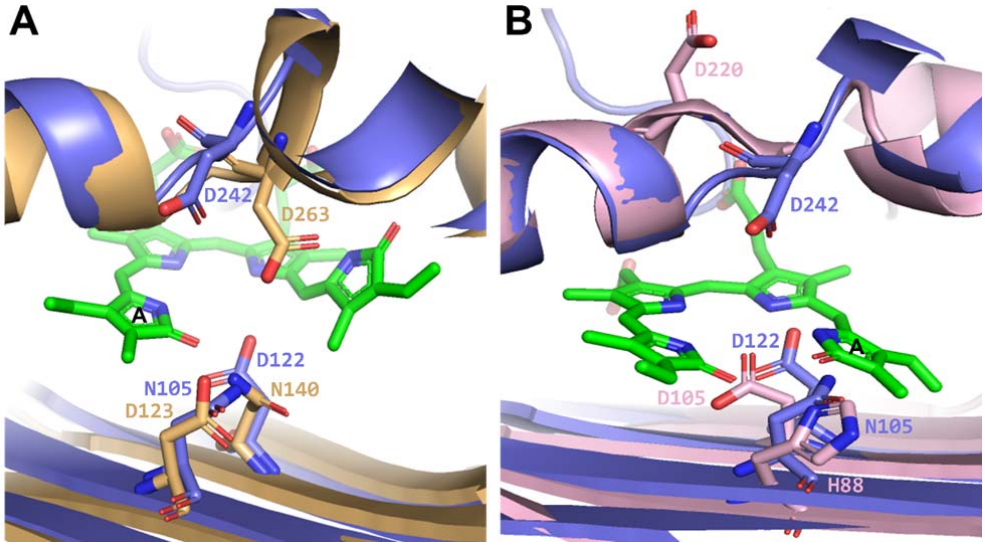

Figure 9 Structures alignment of KflaHY2 with SlHY2 and SynPcyA. The model structure of KflaHY2 (displayed in violet cartoon) was obtained using AlphaFold. The alignments were generated using PyMOL (DeLano, 2020). A. Overlay of the active sites of KflaHY2 and SlHY2. The crystal structure of SlHY2 (PDB accession code: 6KME) is displayed as gold cartoon. Biliverdin IXα, in the conformation assumed in the active site of SlHY2, is shown in green with A-ring being labeled. Amino acid residues of interest are shown as labeled sticks and colored as the belonging structure. B. Overlay of the active sites of KflaHY2 and SynPcyA. The crystal structure of SynPcyA (PDB accession code: 2D1E) is displayed as pink cartoon. Biliverdin IXα, in the conformation assumed in the active site of SlHY2, is shown in green with A-ring being labeled. Amino acid residues of interest are shown as labeled sticks and colored as the belonging structure.

Surprisingly, KflaHY2_N105D_D122N, generated for KflaHY2 to resemble a plant HY2, did not catalyze the hypothesized $2e^-$ reduction of BV to PΦB. Product specificity could then be determined by the architecture of the active site and other residues in the surroundings of the binding pocket. Recently, studies on PcyA proved the replacement of two residues at the rim of the substrate binding pocket determines the accumulation of the $2e^-$ reduced $18^1,18^2$-DHBV as the final product (Miyake et al., 2022). A sequence alignment revealed KflaHY2

426 only possesses a homolog to one of these two PcyA residues. As a following step, the
427 possible involvement of this residue in accumulation of the intermediate in the KflaHY2
428 catalyzed reaction will be investigated. Furthermore, the unexpected outcome of the
429 KflaHY2_N105D_D122N reaction led to the initial assumption that the presence of two
430 aspartate residues in the active site, even if in different position than in the native enzyme, is
431 enough for the reduction of BV to PCB. This hypothesis was disproved by studying the
432 KflaHY2_N105D_D242N variant which, similarly to KflaHY2_N105D, revealed reductase-
433 isomerase activity leading to PEB production. Looking at the model structures of the variants,
434 the formation of either PCB or PEB seemed to be determined by the position of the two
435 aspartate residues in the binding pocket (Figure 10). Indeed, in KflaHY2_N105D and
436 KflaHY2_N105D_D242N only, where the two aspartate residues are laying on the same side
437 of the active site, reductase-isomerase activity could be observed. On the other hand, in
438 KflaHY2 and KflaHY2_N105D_D122N, the two aspartates are opposite to each other,
439 yielding PCB. Ultimately, X-ray crystallography will provide more insights on the catalytic
440 mechanism of KflaHY2.

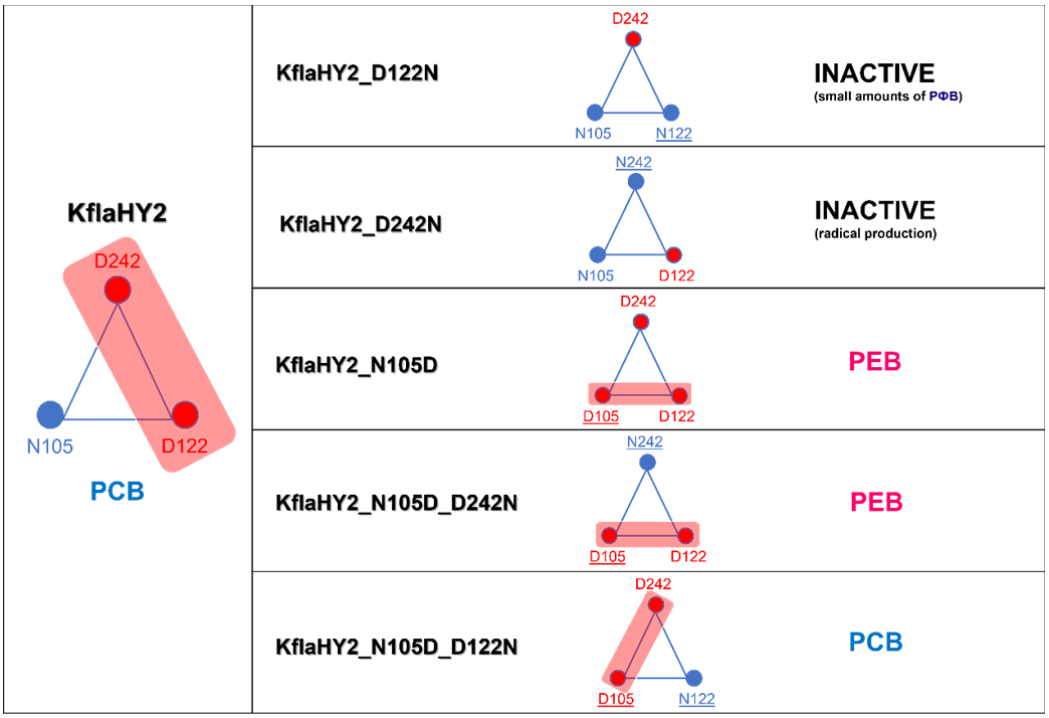

Figure 10 Schematical representation of the active sites and activity of KflaHY2 and its variants. The red box highlights the position of the two aspartate residues. Exchanged residues are underlined. The production of either PCB or PEB is determined by the position of aspartate couple in the active site. Variants in which the aspartate residues are opposite to each other are catalyzing BV reduction to PCB. Variants in which the aspartates are laying on the same side show reductases-isomerase activity, first catalyzing BV reduction to PCB and then isomerizing it to PEB.

Acknowledgement

This project was financially supported by a grant from the Deutsche Forschungsgemeinschaft to NFD. We furthermore thank J. Clark Lagarias for the gift of plasmids and helpful discussions with him and Nathan Rockwell.

Author contributions

FF, BL and NFD designed research, FF, BL, JH performed research, EPP and EH contributed analytical tools, FF, BL and NFD wrote the paper. All authors read and approved the final version of the manuscript.

Conflict of Interest

The authors declare no conflict of interest.

463 # References

464 **Becker B, Marin B** (2009) Streptophyte algae and the origin of embryophytes. Ann Bot. doi:
465 10.1093/aob/mcp044

466 **Busch AWU, Reijerse EJ, Lubitz W, Hofmann E, Frankenberg-Dinkel N** (2011) Radical
467 mechanism of cyanophage phycoerythrobilin synthase (PebS). Biochem J. doi:
468 10.1042/BJ20101642

469 **Cornejo J, Beale SI** (1988) Algal heme oxygenase from Cyanidium caldarium. Partial
470 purification and fractionation into three required protein components. J Biol Chem. doi:
471 10.1016/s0021-9258(18)37873-6

472 **Dammeyer T, Bagby SC, Sullivan MB, Chisholm SW, Frankenberg-Dinkel N** (2008)
473 Efficient Phage-Mediated Pigment Biosynthesis in Oceanic Cyanobacteria. Curr Biol.
474 doi: 10.1016/j.cub.2008.02.067

475 **DeLano WL** (2020) The PyMOL Molecular Graphics System, Version 2.3. Schrödinger LLC

476 **Delwiche CF, Cooper ED** (2015) The evolutionary origin of a terrestrial flora. Curr Biol. doi:
477 10.1016/j.cub.2015.08.029

478 **Fiege K, Frankenberg-Dinkel N** (2020) Construction of a new T7 promoter compatible
479 Escherichia coli Nissle 1917 strain for recombinant production of heme-dependent
480 proteins. Microb Cell Fact. doi: 10.1186/s12934-020-01447-5

481 **Frankenberg N, Lagarias JC** (2003) Phycocyanobilin:ferredoxin oxidoreductase of
482 Anabaena sp. PCC 7120: Biochemical and spectroscopic characterization. J Biol Chem.
483 doi: 10.1074/jbc.M211643200

484 **Frankenberg N, Mukougawa K, Kohchi T, Lagarias JC** (2001) Functional genomic
485 analysis of the HY2 family of ferredoxin-dependent bilin reductases from oxygenic
486 photosynthetic organisms. Plant Cell. doi: 10.1105/tpc.13.4.965

487 **Gill SC, von Hippel PH** (1989) Calculation of protein extinction coefficients from amino acid
488 sequence data. Anal Biochem. doi: 10.1016/0003-2697(89)90602-7

489 **Hagiwara Y, Sugishima M, Khawn H, Kinoshita H, Inomata K, Shang L, Lagarias JC,**
490 **Takahashi Y, Fukuyama K** (2010) Structural insights into vinyl reduction
491 regiospecificity of phycocyanobilin:Ferredoxin oxidoreductase (PcyA). J Biol Chem. doi:
492 10.1074/jbc.M109.055632

493 **Hagiwara Y, Sugishima M, Takahashi Y, Fukuyama K** (2006) Crystal structure of
494 phycocyanobilin:ferredoxin oxidoreductase in complex with biliverdin IXα, a key enzyme
495 in the biosynthesis of phycocyanobilin. Proc Natl Acad Sci U S A. doi:
496 10.1073/pnas.0507266103

497 **Hori K, Maruyama F, Fujisawa T, Togashi T, Yamamoto N, Seo M, Sato S, Yamada T,**
498 **Mori H, Tajima N, et al** (2014) Klebsormidium flaccidum genome reveals primary
499 factors for plant terrestrial adaptation. Nat Commun. doi: 10.1038/ncomms4978

500 **Hu W, Franklin KA, Sharrock RA, Jones MA, Harmer SL, Lagarias JC** (2013)
501 Unanticipated regulatory roles for Arabidopsis phytochromes revealed by null mutant
502 analysis. Proc Natl Acad Sci U S A. doi: 10.1073/pnas.1221738110
503 **Jumper J, Evans R, Pritzel A, Green T, Figurnov M, Ronneberger O, Tunyasuvunakool**
504 **K, Bates R, Žídek A, Potapenko A, et al** (2021) Highly accurate protein structure
505 prediction with AlphaFold. Nature. doi: 10.1038/s41586-021-03819-2
506 **Kohchi T, Mukougawa K, Frankenberg N, Masuda M, Yokota A, Lagarias JC** (2001) The
507 Arabidopsis HY2 gene encodes phytochromobilin synthase, a ferredoxin-dependent
508 biliverdin reductase. Plant Cell. doi: 10.1105/tpc.13.2.425
509 **Ledermann B, Béjà O, Frankenberg-Dinkel N** (2016) New biosynthetic pathway for pink
510 pigments from uncultured oceanic viruses. Environ Microbiol. doi: 10.1111/1462-
511 2920.13290
512 **Li L, Lagarias JC** (1992) Phytochrome assembly. Defining chromophore structural
513 requirements for covalent attachment and photoreversibility. J Biol Chem. doi:
514 10.1016/s0021-9258(18)41762-0
515 **McDowell MT, Lagarias JC** (2001) Purification and biochemical properties of
516 phytochromobilin synthase from etiolated oat seedlings. Plant Physiol. doi:
517 10.1104/pp.126.4.1546
518 **Miyake K, Kimura H, Narikawa R** (2022) Identification of significant residues for
519 intermediate accumulation in phycocyanobilin synthesis. Photochem Photobiol Sci **21**:
520 437–446
521 **Möglich A, Yang X, Ayers RA, Moffat K** (2010) Structure and function of plant
522 photoreceptors. Annu Rev Plant Biol. doi: 10.1146/annurev-arplant-042809-112259
523 **Murphy JT, Lagarias JC** (1997) The phytofluors: A new class of fluorescent protein probes.
524 Curr Biol. doi: 10.1016/S0960-9822(06)00375-7
525 **Rockwell NC, Lagarias JC** (2017) Ferredoxin-dependent bilin reductases in eukaryotic
526 algae: Ubiquity and diversity. J Plant Physiol. doi: 10.1016/j.jplph.2017.05.022
527 **Rockwell NC, Martin SS, Li FW, Mathews S, Lagarias JC** (2017) The phycocyanobilin
528 chromophore of streptophyte algal phytochromes is synthesized by HY2. New Phytol.
529 doi: 10.1111/nph.14422
530 **Sharrock RA** (2008) The phytochrome red/far-red photoreceptor superfamily. Genome Biol.
531 doi: 10.1186/gb-2008-9-8-230
532 **Sommerkamp JA, Frankenberg-Dinkel N, Hofmann E** (2019) Crystal structure of the first
533 eukaryotic bilin reductase GtPEBB reveals a flipped binding mode of dihydrobiliverdin. J
534 Biol Chem. doi: 10.1074/jbc.RA119.009306
535 **Sugishima M, Wada K, Fukuyama K, Yamamoto K** (2020) Crystal structure of
536 phytochromobilin synthase in complex with biliverdin IXα, a key enzyme in the

537 biosynthesis of phytochrome. J Biol Chem. doi: 10.1074/jbc.RA119.011431
538 **Tasler R, Moises T, Frankenberg-Dinkel N** (2005) Biochemical and spectroscopic
539 characterization of the bacterial phytochrome of Pseudomonas aeruginosa. FEBS J.
540 doi: 10.1111/j.1742-4658.2005.04623.x
541 **Tu SL, Chen HC, Ku LW** (2008) Mechanistic studies of the phytochromobilin synthase HY2
542 from Arabidopsis. J Biol Chem. doi: 10.1074/jbc.M803761200
543 **Tu SL, Gunn A, Toney MD, Britt RD, Lagarias JC** (2004) Biliverdin reduction by
544 cyanobacterial phycocyanobilin:ferredoxin oxidoreductase (PcyA) proceeds via linear
545 tetrapyrrole radical intermediates. J Am Chem Soc. doi: 10.1021/ja049280z
546 **de Vries J, Archibald JM** (2018) Plant evolution: landmarks on the path to terrestrial life.
547 New Phytol. doi: 10.1111/nph.14975
548 **Wu SH, McDowell MT, Lagarias JC** (1997) Phycocyanobilin is the natural precursor of the
549 phytochrome chromophore in the green alga Mesotaenium caldariorum. J Biol Chem.
550 doi: 10.1074/jbc.272.41.25700
551 **Xu QZ, Bielytskyi P, Otis J, Lang C, Hughes J, Zhao KH, Losi A, Gärtner W, Song C**
552 (2019) MAS NMR on a red/far-red photochromic cyanobacteriochrome All2699 from
553 Nostoc. Int J Mol Sci. doi: 10.3390/ijms20153656
554

555 # Figure legends

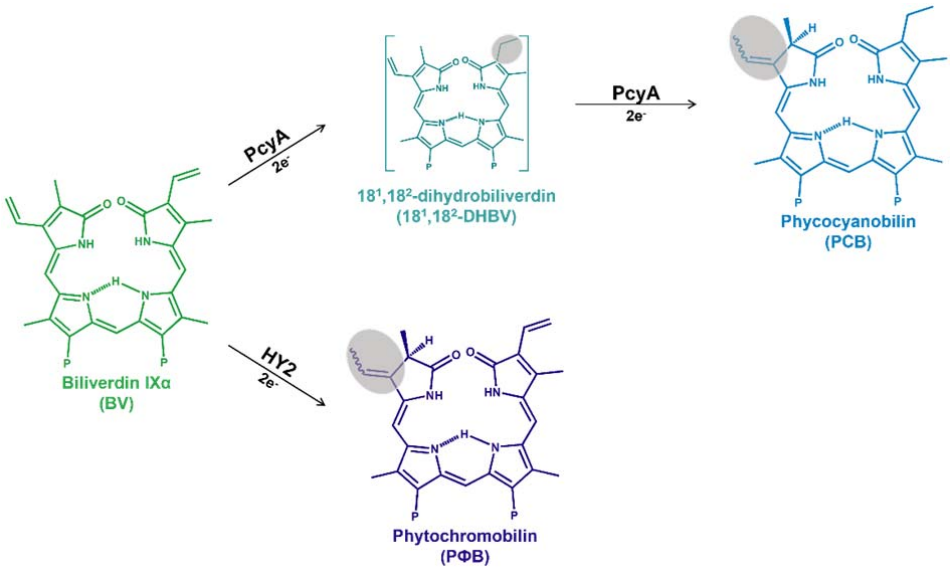

556

557 **Figure 1** Overview of the reactions catalyzed by the FDBRs HY2 and PcyA. Biliverdin IXα (BV) is the substrate of
558 both FDBRs. "P" indicates the propionate side chains. HY2 catalyzes the two-electron reduction of BV to
559 phytochromobilin (PΦB). PcyA catalyzes the four-electron reduction of BV to phycocyanobilin (PCB) via the
560 intermediate 18^1,18^2-dihydrobiliverdin (DHBV). Sites of reduction are highlighted in grey.

561

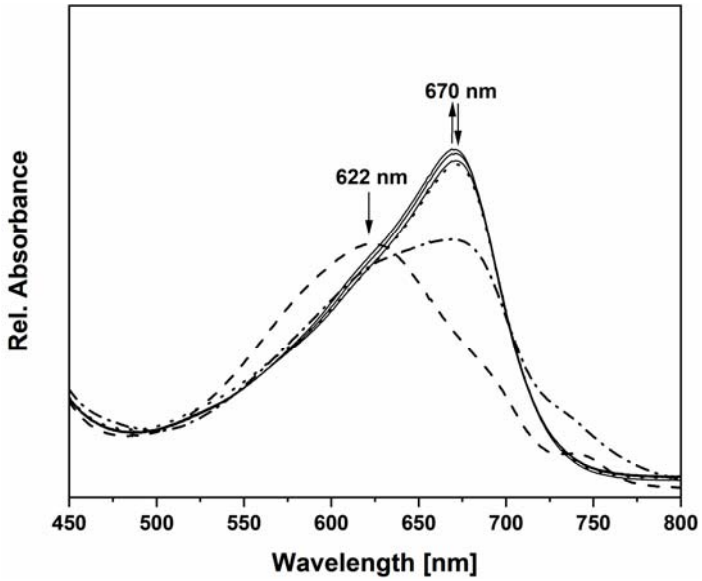

562

563 **Figure 2** Time-resolved UV-Vis spectra of an anaerobic bilin reductase activity test of KflaHY2 employing BV as
564 the substrate. Total reaction time was 5 min and spectra were recorded every 30s. The course of the spectra is
565 marked by arrows. For reasons of clarity, only relevant spectra are shown. The dashed spectrum was acquired
566 without starting the reaction. The dotted-dashed spectrum represents the first acquired after starting the reaction.
567 The dotted curve represents the end spectrum.

568

569

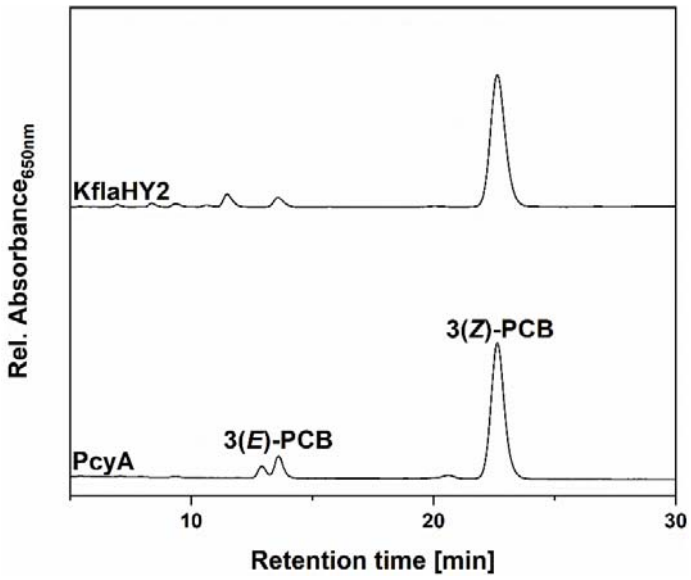

570

571 **Figure 3** HPLC analyses of the reaction products of KflaHY2 with BV as substrate. The products were analyzed
572 using a reversed-phase 5 µm C18 Luna column (Phenomenex) as stationary phase. The mobile phase consisted
573 of 50% (v/v) acetone and 50% (v/v) 20 mM formic acid flowing at 0.6 mL/min. Products of an anaerobic turnover
574 of BV to PCB mediated by PcyA served as standards. Absorbance was continuously measured at 650 nm.

575

576

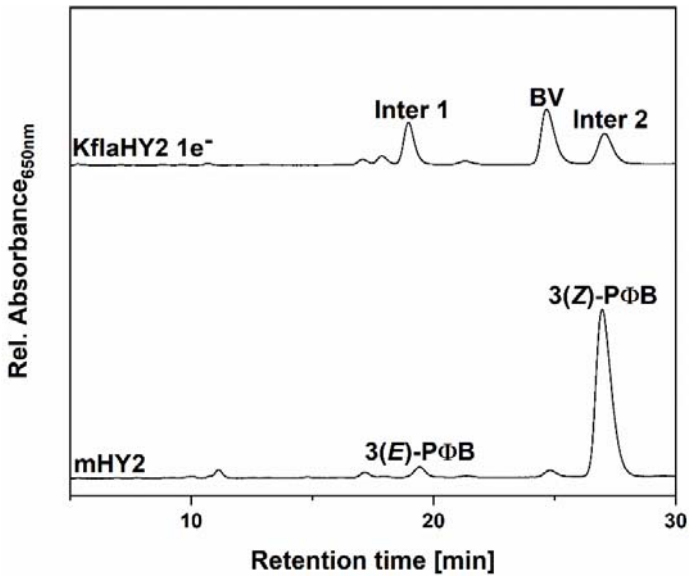

577

578 **Figure 4** HPLC analyses of the reaction products of an anaerobic activity assay employing equimolar amounts of
579 KflaHY2 and BV with one electron equivalent of NADPH. Products were resolved using a reversed-phase 5 µm
580 C18 Luna column (Phenomenex) as stationary phase and a mixture of 50% (v/v) acetone and 50% (v/v) 20 mM
581 formic acid as mobile phase. The products of an anaerobic turnover of BV to PΦB mediated by HY2 derived from
582 *A. thaliana* were used as standards. Absorbance was continuously measured at 650 nm.

583

584

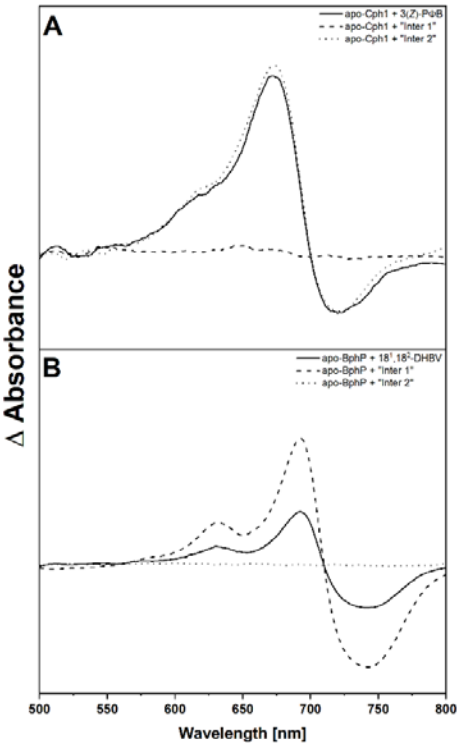

585

586 **Figure 5** Red-far red-light induced difference spectra of coupled phytochrome assembly assays employing the
587 intermediates of the KflaHY2 reaction. Absorbance spectra were recorded after incubation for 3 min with red light
588 (636 nm – Pr spectrum) and after incubation for 3 min with far red light (730 nm for Cph1; 750 nm for BphP – Pfr
589 spectrum). Difference spectra were calculated by the subtraction of the Pfr from the Pr spectrum. All calculated
590 difference spectra were smoothed applying a 20 pt. Savitzky-Golay filter. A Coupled phytochrome assembly
591 assays employing apo-Cph1 and "Inter 1" (dashed line); apo-Cph1 and "Inter 2" (dotted line); apo-Cph1 and 3(*Z*)-
592 PΦB (solid line) B Coupled phytochrome assembly assay employing apo-BphP and "Inter 1" (dashed line); apo-
593 BphP and "Inter 2" (dotted line); apo-BphP and 18^1,18^2-DHBV (solid line).

594

595

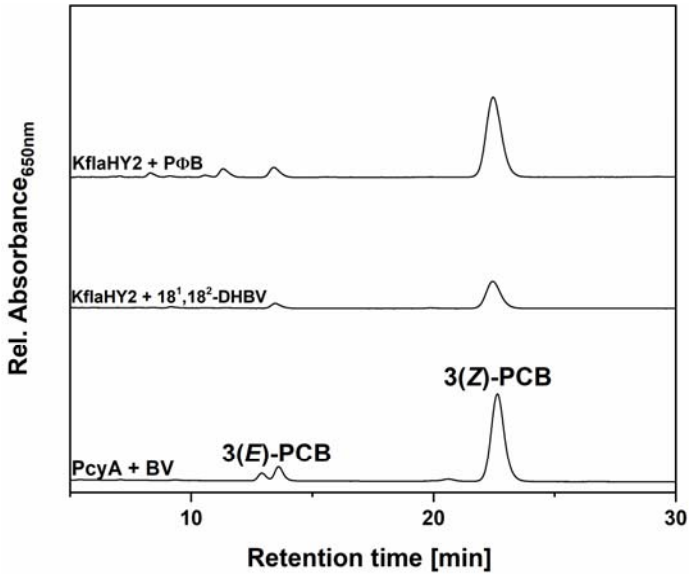

596

597 **Figure 6** HPLC analyses of the reaction products of activity tests employing 3(*Z*)-PΦB and 18^1,18^2-DHBV as
598 substrates for KflaHY2. Products were analyzed using a 5 µm reversed-phase C18 Luna column (Phenomenex)
599 as stationary phase. The mobile phase consisted of 50% (v/v) acetone and 50% (v/v) 20 mM formic acid flowing
600 at 0.6 mL/min. Reaction products of a PcyA mediated reduction of BV to PCB were used as standards.
601 Absorbance was continuously measured at 650 nm.

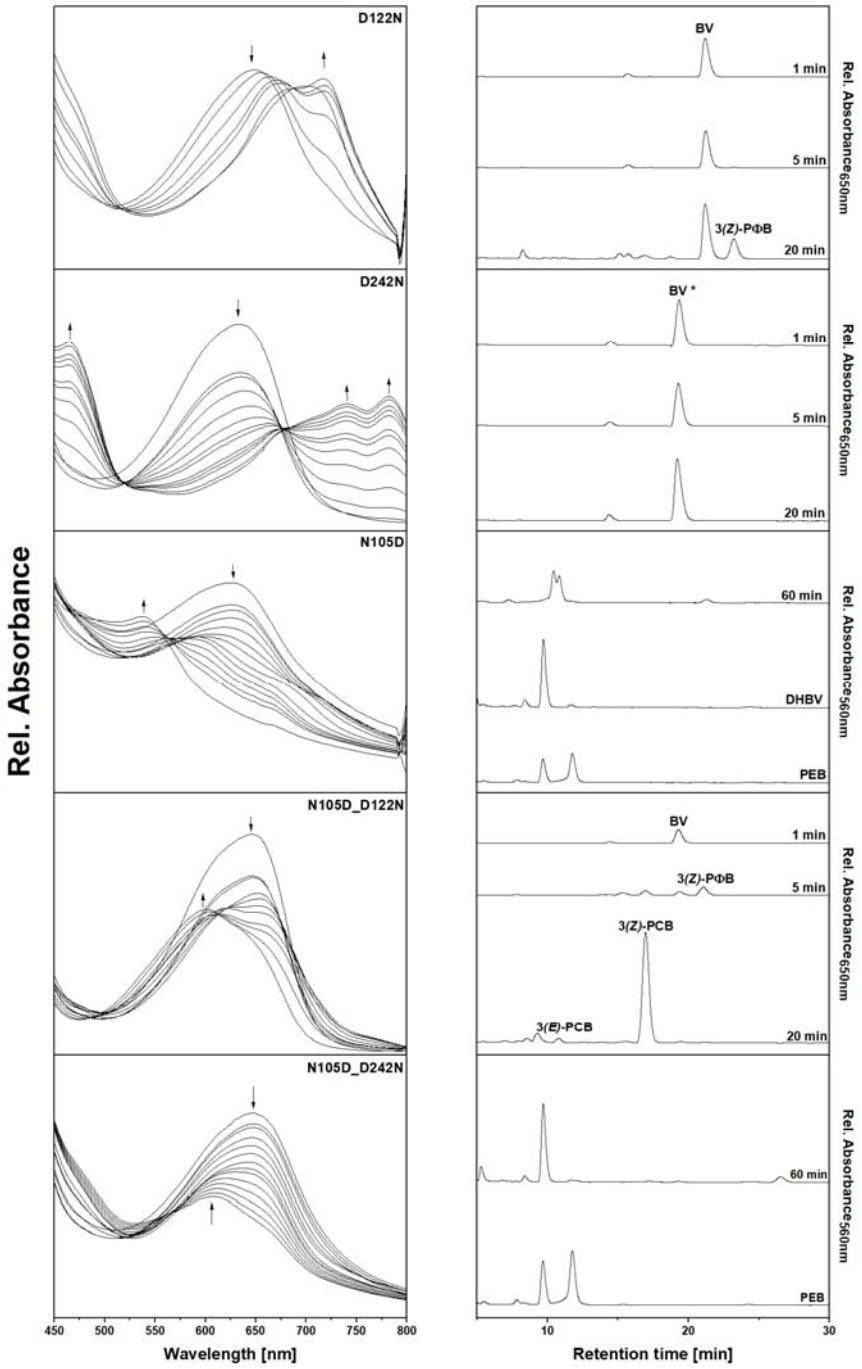

Figure 7 Activity assay and characterization of reaction products of KflaHY2 variants. A UV-Vis spectra of the anaerobic FDBR Assay performed using KflaHY2 variants and BV as the substrate. Total reaction time was 20 minutes for KflaHY2_D122N, KflaHY2_D242N, KflaHY2_N105D_D122N and 60 min for KflaHY2_N105D, KflaHY2_N105D_D242N. Spectra were recorded every 30 seconds. For reasons of clarity, only relevant spectra are shown. The arrow indicates the course of absorbance during the reaction. B HPLC elution profiles of the reaction products of KflaHY2 variants. The stationary phase consisted in a Luna 5µm reversed phase C18 column (Phenomenex). The mobile phase consisted of a mixture of 50% (v/v) acetone and 50% (v/v) 20mM formic acid flowing at 0.6 mL/min. Absorbance was continuously measured at 560 or 650 nm. BV shows change in the retention time due to substitution of the mobile phase between the different HPLC measurements (*).

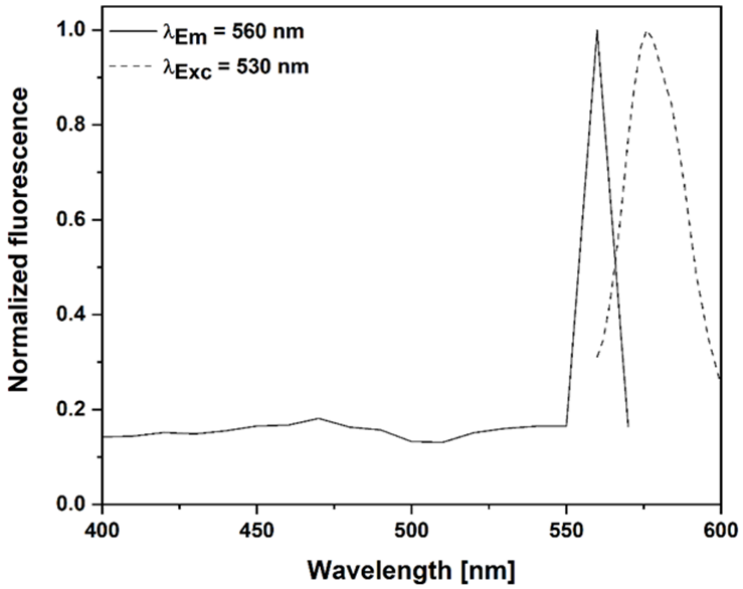

Figure 8 Fluorescence spectra of the apo-Cph1-KflaHY2_N105D reaction product adduct. The isolated bilin produced by KflaHY2_N105D was incubated for 30 min in the dark with the lysate of a pET_*cph1* overproduction. Excitation spectra was obtained at 530 nm. Fluorescence emission was recorded after excitation at 560 nm.

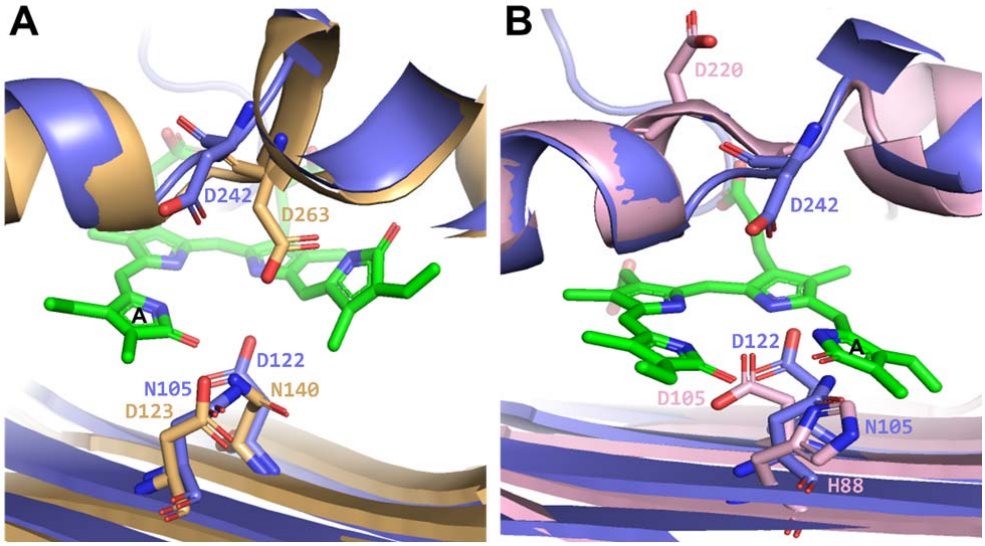

Figure 9 Structures alignment of KflaHY2 with SlHY2 and SynPcyA. The model structure of KflaHY2 (displayed in violet cartoon) was obtained using AlphaFold. The alignments were generated using PyMOL (DeLano, 2020). A. Overlay of the active sites of KflaHY2 and SlHY2. The crystal structure of SlHY2 (PDB accession code: 6KME) is displayed as gold cartoon. Biliverdin IXα, in the conformation assumed in the active site of SlHY2, is shown in green with A-ring being labeled. Amino acid residues of interest are shown as labeled sticks and colored as the belonging structure. B. Overlay of the active sites of KflaHY2 and SynPcyA. The crystal structure of SynPcyA (PDB accession code: 2D1E) is displayed as pink cartoon. Biliverdin IXα, in the conformation assumed in the active site of SlHY2, is shown in green with A-ring being labeled. Amino acid residues of interest are shown as labeled sticks and colored as the belonging structure.

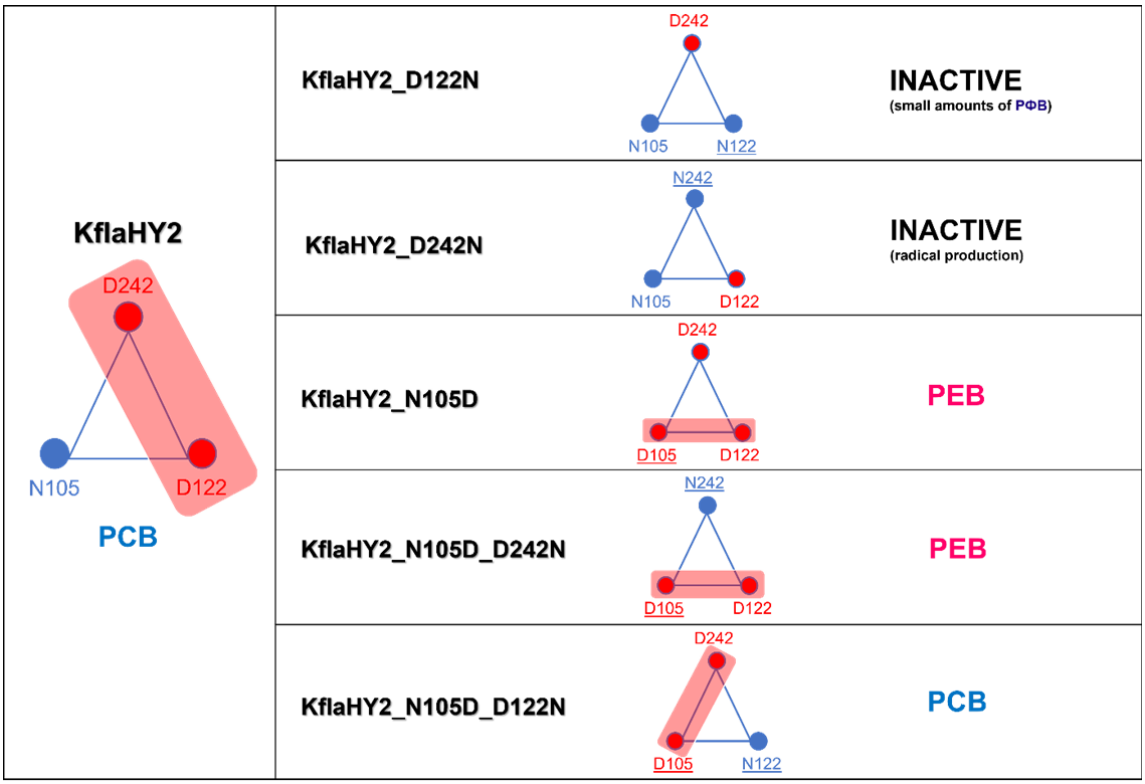

Figure 10 Schematical representation of the active sites and activity of KflaHY2 and its variants. The red box highlights the position of the two aspartate residues. Exchanged residues are underlined. The production of either PCB or PEB is determined by the position of aspartate couple in the active site. Variants in which the aspartate residues are opposite to each other are catalyzing BV reduction to PCB. Variants in which the aspartates are laying on the same side show reductases-isomerase activity, first catalyzing BV reduction to PCB and then isomerizing it to PEB.

Parsed Citations

Becker B, Marin B (2009) Streptophyte algae and the origin of embryophytes. Ann Bot. doi: 10.1093/aob/mcp044
Google Scholar: Author Only Title Only Author and Title

Busch AWU, Reijerse EJ, Lubitz W, Hofmann E, Frankenberg-Dinkel N (2011) Radical mechanism of cyanophage phycoerythrobilin synthase (PebS). Biochem J. doi: 10.1042/BJ20101642
Google Scholar: Author Only Title Only Author and Title

Cornejo J, Beale SI (1988) Algal heme oxygenase from Cyanidium caldarium. Partial purification and fractionation into three required protein components. J Biol Chem. doi: 10.1016/s0021-9258(18)37873-6
Google Scholar: Author Only Title Only Author and Title

Dammeyer T, Bagby SC, Sullivan MB, Chisholm SW, Frankenberg-Dinkel N (2008) Efficient Phage-Mediated Pigment Biosynthesis in Oceanic Cyanobacteria. Curr Biol. doi: 10.1016/j.cub.2008.02.067
Google Scholar: Author Only Title Only Author and Title

DeLano WL (2020) The PyMOL Molecular Graphics System, Version 2.3. Schrödinger LLC
Google Scholar: Author Only Title Only Author and Title

Delwiche CF, Cooper ED (2015) The evolutionary origin of a terrestrial flora. Curr Biol. doi: 10.1016/j.cub.2015.08.029
Google Scholar: Author Only Title Only Author and Title

Fiege K, Frankenberg-Dinkel N (2020) Construction of a new T7 promoter compatible Escherichia coli Nissle 1917 strain for recombinant production of heme-dependent proteins. Microb Cell Fact. doi: 10.1186/s12934-020-01447-5
Google Scholar: Author Only Title Only Author and Title

Frankenberg N, Lagarias JC (2003) Phycocyanobilin:ferredoxin oxidoreductase of Anabaena sp. PCC 7120: Biochemical and spectroscopic characterization. J Biol Chem. doi: 10.1074/jbc.M211643200
Google Scholar: Author Only Title Only Author and Title

Frankenberg N, Mukougawa K, Kohchi T, Lagarias JC (2001) Functional genomic analysis of the HY2 family of ferredoxin-dependent bilin reductases from oxygenic photosynthetic organisms. Plant Cell. doi: 10.1105/tpc.13.4.965
Google Scholar: Author Only Title Only Author and Title

Gill SC, von Hippel PH (1989) Calculation of protein extinction coefficients from amino acid sequence data. Anal Biochem. doi: 10.1016/0003-2697(89)90602-7
Google Scholar: Author Only Title Only Author and Title

Hagiwara Y, Sugishima M, Khawn H, Kinoshita H, Inomata K, Shang L, Lagarias JC, Takahashi Y, Fukuyama K (2010) Structural insights into vinyl reduction regiospecificity of phycocyanobilin:Ferredoxin oxidoreductase (PcyA). J Biol Chem. doi: 10.1074/jbc.M109.055632
Google Scholar: Author Only Title Only Author and Title

Hagiwara Y, Sugishima M, Takahashi Y, Fukuyama K (2006) Crystal structure of phycocyanobilin:ferredoxin oxidoreductase in complex with biliverdin IXα, a key enzyme in the biosynthesis of phycocyanobilin. Proc Natl Acad Sci U S A. doi: 10.1073/pnas.0507266103
Google Scholar: Author Only Title Only Author and Title

Hori K, Maruyama F, Fujisawa T, Togashi T, Yamamoto N, Seo M, Sato S, Yamada T, Mori H, Tajima N, et al (2014) Klebsormidium flaccidum genome reveals primary factors for plant terrestrial adaptation. Nat Commun. doi: 10.1038/ncomms4978
Google Scholar: Author Only Title Only Author and Title

Hu W, Franklin KA, Sharrock RA, Jones MA, Harmer SL, Lagarias JC (2013) Unanticipated regulatory roles for Arabidopsis phytochromes revealed by null mutant analysis. Proc Natl Acad Sci U S A. doi: 10.1073/pnas.1221738110
Google Scholar: Author Only Title Only Author and Title

Jumper J, Evans R, Pritzel A, Green T, Figurnov M, Ronneberger O, Tunyasuvunakool K, Bates R, Žídek A, Potapenko A, et al (2021) Highly accurate protein structure prediction with AlphaFold. Nature. doi: 10.1038/s41586-021-03819-2
Google Scholar: Author Only Title Only Author and Title

Kohchi T, Mukougawa K, Frankenberg N, Masuda M, Yokota A, Lagarias JC (2001) The Arabidopsis HY2 gene encodes phytochromobilin synthase, a ferredoxin-dependent biliverdin reductase. Plant Cell. doi: 10.1105/tpc.13.2.425
Google Scholar: Author Only Title Only Author and Title

Ledermann B, Béjà O, Frankenberg-Dinkel N (2016) New biosynthetic pathway for pink pigments from uncultured oceanic viruses. Environ Microbiol. doi: 10.1111/1462-2920.13290
Google Scholar: Author Only Title Only Author and Title

Li L, Lagarias JC (1992) Phytochrome assembly. Defining chromophore structural requirements for covalent attachment and

photoreversibility. J Biol Chem. doi: 10.1016/s0021-9258(18)41762-0
Google Scholar: Author Only Title Only Author and Title

McDowell MT, Lagarias JC (2001) Purification and biochemical properties of phytochromobilin synthase from etiolated oat seedlings. Plant Physiol. doi: 10.1104/pp.126.4.1546
Google Scholar: Author Only Title Only Author and Title

Miyake K, Kimura H, Narikawa R (2022) Identification of significant residues for intermediate accumulation in phycocyanobilin synthesis. Photochem Photobiol Sci 21: 437–446
Google Scholar: Author Only Title Only Author and Title

Möglich A, Yang X, Ayers RA, Moffat K (2010) Structure and function of plant photoreceptors. Annu Rev Plant Biol. doi: 10.1146/annurev-arplant-042809-112259
Google Scholar: Author Only Title Only Author and Title

Murphy JT, Lagarias JC (1997) The phytofluors: A new class of fluorescent protein probes. Curr Biol. doi: 10.1016/S0960-9822(06)00375-7
Google Scholar: Author Only Title Only Author and Title

Rockwell NC, Lagarias JC (2017) Ferredoxin-dependent bilin reductases in eukaryotic algae: Ubiquity and diversity. J Plant Physiol. doi: 10.1016/j.jplph.2017.05.022
Google Scholar: Author Only Title Only Author and Title

Rockwell NC, Martin SS, Li FW, Mathews S, Lagarias JC (2017) The phycocyanobilin chromophore of streptophyte algal phytochromes is synthesized by HY2. New Phytol. doi: 10.1111/nph.14422
Google Scholar: Author Only Title Only Author and Title

Sharrock RA (2008) The phytochrome red/far-red photoreceptor superfamily. Genome Biol. doi: 10.1186/gb-2008-9-8-230
Google Scholar: Author Only Title Only Author and Title

Sommerkamp JA, Frankenberg-Dinkel N, Hofmann E (2019) Crystal structure of the first eukaryotic bilin reductase GtPEBB reveals a flipped binding mode of dihydrobiliverdin. J Biol Chem. doi: 10.1074/jbc.RA119.009306
Google Scholar: Author Only Title Only Author and Title

Sugishima M, Wada K, Fukuyama K, Yamamoto K (2020) Crystal structure of phytochromobilin synthase in complex with biliverdin IXα, a key enzyme in the biosynthesis of phytochrome. J Biol Chem. doi: 10.1074/jbc.RA119.011431
Google Scholar: Author Only Title Only Author and Title

Tasler R, Moises T, Frankenberg-Dinkel N (2005) Biochemical and spectroscopic characterization of the bacterial phytochrome of Pseudomonas aeruginosa. FEBS J. doi: 10.1111/j.1742-4658.2005.04623.x
Google Scholar: Author Only Title Only Author and Title

Tu SL, Chen HC, Ku LW (2008) Mechanistic studies of the phytochromobilin synthase HY2 from Arabidopsis. J Biol Chem. doi: 10.1074/jbc.M803761200
Google Scholar: Author Only Title Only Author and Title

Tu SL, Gunn A, Toney MD, Britt RD, Lagarias JC (2004) Biliverdin reduction by cyanobacterial phycocyanobilin:ferredoxin oxidoreductase (PcyA) proceeds via linear tetrapyrrole radical intermediates. J Am Chem Soc. doi: 10.1021/ja049280z
Google Scholar: Author Only Title Only Author and Title

de Vries J, Archibald JM (2018) Plant evolution: landmarks on the path to terrestrial life. New Phytol. doi: 10.1111/nph.14975
Google Scholar: Author Only Title Only Author and Title

Wu SH, McDowell MT, Lagarias JC (1997) Phycocyanobilin is the natural precursor of the phytochrome chromophore in the green alga Mesotaenium caldariorum. J Biol Chem. doi: 10.1074/jbc.272.41.25700
Google Scholar: Author Only Title Only Author and Title

Xu QZ, Bielytskyi P, Otis J, Lang C, Hughes J, Zhao KH, Losi A, Gärtner W, Song C (2019) MAS NMR on a red/far-red photochromic cyanobacteriochrome All2699 from Nostoc. Int J Mol Sci. doi: 10.3390/ijms20153656
Google Scholar: Author Only Title Only Author and Title